Int J Clin Exp Med 2019;12(8):10399-10410
www.ijcem.com /ISSN:1940-5901/IJCEM0094769

Original Article

Influence of location of osseointegrated implant on stress distribution in implant supported longitudinal removable partial dentures: 3-dimensional finite element analysis

Yang Liu[1], Yi-Nan Zhang[2], Keiichi Sasaki[3], Xiao-Dong Chen[1]

[1]*Department of Prosthodontics, Dalian Stomatological Hospital, Dalian, China;* [2]*Graduate School of Dentistry, Dalian Medical University, Dalian, China;* [3]*Division of Advanced Prosthetic Dentistry, Graduate School of Dentistry, Tohoku University, Sendai, Japan*

Received April 2, 2019; Accepted July 10, 2019; Epub August 15, 2019; Published August 30, 2019

Abstract: Unilateral distal extension partial dentures supported by longitudinal fulcrum lines tend to rotate and sink, while adding an implant support has been found to help improve stability. The purpose of this study was to evaluate the biomechanical behavior of a mandibular distal extension removable partial denture associated with an implant, including its difference in the distribution of stress within the bone, alveolar mucosa, and implants, as well as investigating the displacement of alveolar mucosa and RPD using the 3-dimensional finite element method. The results show that, with or without implant support, stress concentrations occur in the buccal side of the alveolar ridge in the premolar area. Using implants to support the RPD can reduce the Von Mises stress on the cortical bone and alveolar mucosa. This also reduces the deformation of the denture and alveolar mucosa, and increases the Von Mises stress of the cancellous bone under load. Moreover, under the functional load, the dentures are prone to uneven deformation, but this deformation occurs in a mistal retainer that is supported by the implant, denture displacement is reduced and the deformation becomes uniform. As the implant grows farther and farther away, the support for the premolar area is gradually eased and support for the molar area increases. The implant bears the majority of a given functional load. We conclude that, in the premolar area, the implant effectively disperses the force and reduces the stress value of the cortical bone, while in the molar area, the cortical bone takes more occlusal force and the implant is protected.

Keywords: Kennedy II, longitudinal, implant, removable partial denture, 3-D FEA

Introduction

Conventional Removable Partial Dentures (CRPD) are often used to repair Kennedy class II dentition defects with unilateral distal extension absences. As a result of the dissimilarity of the periodontal ligament of the abutment teeth and the mucosa, and also the differences in separability, the denture base sinks towards the tissue under the action of the occlusal force, leading to the occurrence of instability such as rotational motion in which the end abutment teeth serve as a fulcrum. In addition, the setting of an indirect retainer on the opposite side of the fulcrum line is likely to result in damage to the abutment teeth. If long-term use of a distal extension RPD is made, this will create constant pressure on the abutment teeth and tissue, as well as permanently affect the absorption of the alveolar ridge in the edentulous area. This will inevitably result in abutment loosening, poor retention, and stability issues, and also low chewing efficiency [1]. Further, as the molars and premolars are missing, the center of the occlusal force will often gradually move toward the mistal direction. The loss of occlusal contact at the distal extension often leads to temporomandibular joint syndrome.

In the division of RPD, Wang Zhengshou [2] described a sixth category in which most or all of the teeth on one side of the arch are missing, the abutment teeth are all on the other side of the arch, and the abutment teeth side may also have anodontia as a result of the design of the dentures, while the teeth may be out of position and have a number of gaps. In this situation, the retainer is usually placed on the opposite side of the edentate arch to form a partial denture supported by the longitudinal fulcrum line. This method is prone to buccal and lingual rotation along the front and back rotation axis of the denture, and can lead to even more severe instability. Although Xu Jun [3] proposed the idea of placing the retention arm on the lingual side in such cases, this may ameliorate the force placed on the abutment, it puts yet higher demands on the alveolar ridge and the mucosa. Therefore, it is necessary to pay more attention to the repair and stress distribution of longitudinal partial dentures for Kennedy class-II dentition defects.

In recent years, a combination of implants and partial dentures has been used to repair distal extension absences, providing a new treatment option for patients in these cases. The support of the implant can effectively disperse the occlusa force of abutment teeth and tissue, reduce bone resorption, prolong the life of abutment teeth, and thus provide better stability and preservation of both soft and hard tissues. Some studies [4-6] have shown that even a short implant can provide support for distally extension removable partial dentures and it is expected to reduce overload. Rocha [7] also reached the same conclusion. In one *in-vitro* experiment, Maki [8] measured the difference between the displacement of the denture and the stress on the soft tissue based on distal extension RPDs with and without the assistance of an implant. The results showed that the displacement and stress of implant-assisted dentures were significantly smaller than those of conventional partial dentures. It was therefore proved that the placement of the implant can prevent the displacement of distal extension partial dentures and reduce the resulting pressure on the soft tissue. Grossmann et al [9-11] recommended using the second molar position of the implant to enhance support and stability, while placing the implant near the distal abutment event left of the posterior alveolar ridge in bad condition. Compared with CRPD, implant-supported removable partial denture (ISRPD) can be designed to have a smaller denture support area and provide much more comfort for patients. Therefore, an implant can appropriately reduce the area of the denture base, reduce the number of clasps, improve aesthetic effect and chewing efficiency, and produce a better self-cleaning performance, which is beneficial to the maintenance of oral hygiene. Kuzmanovic et al [12] had a significant effect on Kennedy class-I edentulous cases with removable dentures and bilateral posterior implants. No complications were found during 2 years of follow-up. In an *in-vivo* experimental study [13] on implant-assisted partial dentures, it was concluded that implant-assisted RPDs perform better in terms of comfort, chewing efficiency, retention, and stability than traditional dentures.

In clinical use, the longitudinal partial dentures show great instability, as well as being difficult to repair and showing poor restoration effects. Further, there are only a small number of related studies of basic research and clinical research in this field, suggesting its great degree of difficulty. This study uses the research object of Kennedy class-II dentition defects involving the loss of most unilateral teeth. The implant is placed into the distal-extension absent alveolar ridge to support the longitudinal denture in an attempt to change the linear support of the longitudinal denture to a surface support, thereby increasing stability. The paper then goes on to analyze and discuss the stress distribution of these implant-assisted longitudinal partial dentures through the use of finite element analysis (FEA) in an attempt to further examine the safety and stability of the implant and the health of the tissue. This is done to provide reference for related research and work in the future.

Materials and methods

Experimental materials and equipment

Hardware: KaVo 3D eXam, KaVo Inc., German CT scanner; Dell commercial desktop, 64 GB processor memory, 128 GB hard disk, Windows 7 64-bit operating system.

Soft tissue horizontal implant, standard neck, diameter of 4.1 mm, length of 10 mm. Height of healing base platform: 2 mm.

Software: Mimics 17 (Materialise, Inc.); Geomagic Studio 2012 (Geomagic, Inc.); Hypermesh 12.0 (Altair, Inc.); Abaqus 6.13 (SIMULIA, Inc.).

Table 1. Group of Experiments

	Number	Position
①	0	Blank control
②	0	CRPD
③	1	#4
④	1	#5
⑤	1	#6
⑥	1	#7

Models

Six models of mandibular unilateral partially edentulous models missing the canine to the second molar were created using Computer-Aided Design (CAD) modeling based on patients' images.

A set of 4.1×10 mm implants (Standard RN; Straumann AG, Basel, Switzerland) were inserted in the edentulous residual ridge vertical to the occlusal plane. A healing abutment was placed on the implant so that 2 mm of the abutment protruded from the soft tissue, and came in direct contact with the resin.

The experimental ISRPD consisted of a cobalt–chromium alloy metal frame equipped with two A-ker clasps on the opposite arch as a direct retainer for the left first premolar and third molar, and acrylic resin for the denture base material. The major connector was designed as a lingual plate. The bracing and supporting elements were designed so that the plate came in contact with the anterior tooth. The artificial teeth were also made from the same base material as the denture and were fabricated parallel to the occlusal plane.

The implants were numbered and divided into groups 0 and 1, which simulated a blank control group with no implants and no dentures, an ordinary control group without implants but with traditional partial dentures, and patients who had an implant located in different positions. Details of Models ① to ⑥ are shown in the adjacent table (**Table 1**).

Experimental methods

Data acquisition: In 2017, research subjects were selected from a group of patients in the prosthodontics department of Dalian Stomatological Hospital who wished to receive implant-supported partial denture treatments. The patients did not receive invasive treatment within 6 months before surgery, and denied all histories of major relevant medical conditions and drug allergies. Implants were placed in their right mandibular molar area, and CBCT was taken before and after surgery.

Craniofacial axial tomography was performed on the test subjects with a resolution of 0. 2 mm, mAs=20.27, KVP=120, and with an acquisition time of 14.7 seconds. The patients were seated and the orbital plane was parallel to the horizontal plane. Because the metal part of the denture affects CT imaging, the patient's intraoral plaster model has been reproduced to keep the dentures in place. 3D scanning was conducted on the plaster model of the denture. The scanned images were then processed and saved in STL format.

Establishing geometric models of mandibles and dentures: The research group then reviewed DICOM data obtained via CT scanning of the mandible through Mimics 17.0 3D, the medical reconstruction software. A point cloud region was generated for the mandible by setting thresholds within the range of the bone, determining the thickness of the cancellous bone, cortical bone, and mucous membrane through processes such as erosion and expansion, and then using these models to generate corresponding 3D point cloud models.

To model the denture components, the models' outer contours of the denture were scanned using the handheld scanning device 3 shape, resulting in a file containing point cloud information in STL format.

The exported STL file is then imported into reverse-engineering software Geomagic Studio 2012 to generate a 2D facet. The geometric discontinuous features were then processed by using the grid doctor function, removing irregular and abrupt geometric features through a sequence of surface selections, filling, deletions, noise reduction, point-surface transformation, and other functions to generate a smooth NURB curved surface. The curved surface was then optimized and packaged to make the 3D model more accurate and workable, ending in the generation and export of the geometry in IGES format.

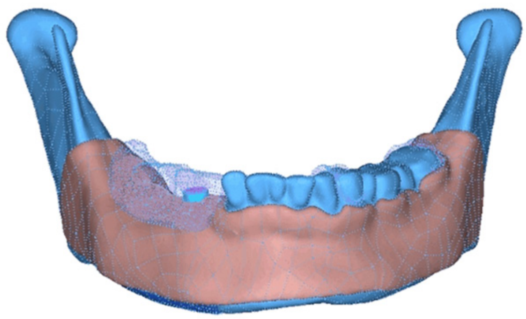

Figure 1. Assemble an implant to the diagram.

Establishing a 3D geometric model of the implant system: The implant, central screw, and abutment are then physically mapped using a digital caliper, creating a 3D geometric model of the implant system using UG software in combination with the parameters provided by the manufacturer, exporting the model in IGES format.

Establishing a 3D finite element model: The mandible model and implant system model established above are then imported into the finite element pre-processing software Hypermesh in IGES format, after which the previously established curved surface model is stitched to establish and assemble a solid model. The geometric part is cut through Boolean operations, and the implant is embedded into the mandible to create a mandibular model containing an implant, and a review is performed to ensure that there is no interference between the different parts.

The model is divided into meshes and the length-width ratio of the element and the jacobi matrix is checked through the tetrahedron element to ensure the continuity of the element.

The final meshes are then smoothed and assigned corresponding material properties, such as elasticity modulus and density. The contact faces of each part as set a separate face set and exported together with the element model (**Figure 1**).

Finite element pre-processing: Static analysis steps are then created, setting the contact surfaces between cancellous bone and cortical bone, cortical bone and mucous membrane, mucous membrane and denture, denture and implant, implant and mandible, etc. The parameters are then adjusted in the contact settings to enable iterative convergence of the analysis steps. The implant is then connected to various parts of the mandible and is set to be 100% bound to the bone.

The node set and face set are then set (**Table 2**), and used to calculate by the C3D4 element. As for the device load and boundary conditions, vertical downward pressure is applied to the upper part of the denture, constraining both sides of the mandible and calculating the force and stress distribution of the overall model.

Hypothesis of mechanical parameters and experimental conditions of the material

Various materials and tissues in the model are identified and marked as continuous, homogeneous, and isotropic linear elastic materials. The implant-bone interface is completely bonded, and thus no relative sliding will occur during loading.

The elastic modulus and Poisson's ratio of the material are obtained based on previous literature [14-16]. See **Table 3**.

Loading conditions and constraint conditions

Boundary conditions: Assume that the bone-mucosa interface, implant-bone interface, and the interface between the implant and the upper abutment are continuous and rigid interfaces free from relative displacement. The implant and the denture are in contact with each other through metal, and the mucosa-denture tissue surfaces are in contact with one another, allowing for vertical displacement. The left and right sides of the mandible and the bottom cortical bone are fixed in all directions to prevent lateral movement. The denture, mucosa, and bone are allowed to move in the Y-axis direction, thereby simulating the displacement of the denture and the deformation of the mucosa and bone.

Loading conditions: The center of the joint of the mandible 33, 34, 35, 36, and 37 are selected as the loading points and loaded vertically with a loading force of 50 Newtons. The same load is applied to all six models in an evenly distributed manner (**Figure 2**).

Statistical methodology

The statistical method of this paper uses random block analysis of variance, and the LSD method is used for comparison between

Table 2. The number of nodes and units in the experimental mode

	1	2	3	4	5	6
Nodes	17067	18492	18937	18983	18987	18988

Table 3. Material mechanics parameter

Part	Elastic Modulus	Poisson's ratio
Implant	107000	0.33
Cortical bone	13700	0.30
Cancellous bone	1370	0.30
Periodontal ligament	69	0.45
Mucosa	3	0.45
Natural tooth	20290	0.3
Denture base	2352	0.33

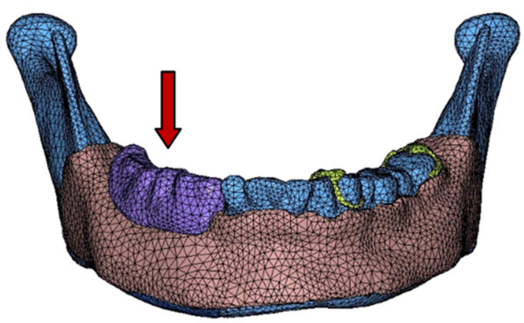

Figure 2. Diagram of loading conditions.

groups. The results suggest that there is a significant difference in the pressure of different tissues F=9.670, P<0.001. The pressure of cortical bone (10-1 MPa) is significantly higher than that of other tissues. There is no significant difference in pressure between the other tissues. There was a significant difference in pressure between different parts F=5.603, P=0.001. Comparison between groups showed that the pressure in the blank control group was significantly lower than that in CRPD, #4, #5, #6, and #7, and there was no significant difference between other parts (**Tables 4**, **5**).

Result

Implants

(1) From the stress cloud diagrams, it can be seen that the maximum stress is concentrated on the neck and 1/3 of the root of the implant. The maximum stress in these areas occurred when the implant is at #5. The stress trends show that when the implant moved towards the distal side, the stress on the root of the implant gradually decreased, while that on the neck increased.

(2) It can be seen from the Von Mises stress value chart (**Figure 3**) that the implant bore greater stress when it was placed on the premolars than on the molars. The maximum value exists at #5, while the minimum exists at #7.

Cortical bone

(1) Evaluating the stress cloud diagrams, and comparing them with the blank control group, the CRPD group mainly focused on the alveolar buccal side of the premolar area. The maximum stress is $8.917*10^{-1}$ MPa.

(2) After placing an implant, the maximum stress was smaller than the corresponding area of the CRPD group, both in the premolar area and the molar area.

(3) It can be seen from the Von Mises stress value chart (**Figure 3**) that when the implant is at #5, the stress value is at its maximum, while at #6, the stress value is the smallest.

Cancellous bone

(1) From the stress cloud diagrams, it can be seen that when comparing the CRPD group with the blank control group, the cancellous bone in the edentulous area is heavily stressed, and the stress is mainly concentrated on the buccal side of the alveolar ridge in the premolar area. The maximum stress is $1.098*10^{-1}$ MPa. High stress appears in the premolar area, and low stress in the molar area. The former stress value is about 2 times larger than the latter.

(2) From the stress cloud diagrams, the stress in the premolar area or the molar area was less than that in the CRPD group after implant support. As the implant moves to the distal end, the stress in the premolar region gradually increases, and the stress in the molar region gradually decreases.

(3) However, examining the Von Mises stress value (**Figure 3**), the maximum stress of cancellous bone with an implant support is greater than that without an implant, and as the implant moves to the distal end, the maximum value gradually decreases.

Table 4. Result data

	Blank Control	CRPD	#4	#5	#6	#7
Implant (MPa)	0	0.000	1.654	1.736	1.316	0.972
Cortical bone (10-1 MPa)	0	8.917	4.980	5.652	4.950	5.460
Cancellous bone (10-1 MPa)	0	1.098	4.221	3.167	2.362	1.524
Mucosa stress (10-1 MPa)	0	2.516	2.045	2.415	1.620	1.583
Mucosa displacement (10-3 MPa)	0	1.108	0.944	1.448	1.433	1.419
Denture negative displacement (10-3 Mpa)	0	1.351	1.249	1.733	1.734	1.713
Denture positive displacement (10-4 MPa)	0	3.150	2.432	1.287	1.758	0.455

Mucosa

(1) Looking at the mucosa deformation and stress distribution maps, the stress is concentrated on the buccal side of the premolar region. In the edentulous area, the mucosa mainly shows compressive stress, while in the contralateral arch, the mucosa shows tensile stress.

(2) Maximum displacement also occurs in the premolar area.

(3) From the Von Mises stress tables (**Figure 3**), it can be seen that the maximal stress of the implant-supported mucosa was less than in those without implant support.

(4) The maximum value appears when the implant is at #5, at which time the mucosa deformation is greatest. When the implant is at #7, the maximum stress on the mucosa is minimal.

(5) In terms of the maximum value of mucosa displacement deformation (**Figure 3**), except in the #4 group which had results slightly smaller than the CRPD group, all showed the other groups to be larger than the control group.

Displacement of denture framework

(1) Examining the denture displacement diagrams, the denture base is expressed as undergoing compressive stress, and the retainer shows tensile stress, while the maximum deformation occurs on the mistal clasp of the metal bracket.

(2) In terms of the displacement of the denture base, maximum displacement appeared on the buccal side of the premolar area, except for #4 which had results slightly smaller than the CRPD group, while other groups were slightly larger than those of control group. The Von Mises stress value shows that the denture base displacement tends to increase as the implant moves distally.

(3) In terms of the displacement of the contralateral retainer: the stress cloud maps show that the displacement of the implant-supported retainers are more uniform than that of the control group. The Von Mises stress value shows (**Figure 3**) that as the implant moves distally, the displacement of the retainer tends to decrease.

Discussion

Impact of implant support on sustentacular tissue and dentures

The functional state of conventional removable partial dentures (CRPD) suggested that there were large differences in alveolar ridge stress and mucosa displacement in the premolar area and the molar area of the CRPD group, with stress concentrated on the mesial clasp in the denture retainer, indicating that the distal denture base had sunk unevenly and compressed the tissues, as well as placing a large load on the abutment teeth. This coincides with the opinions of many scholars. For example, some researchers [7, 15, 17] believed that the CRPD made the edges of the alveolar ridge and the abutment teeth overloaded, which may lead to the potential destruction of these tissues. These results suggest that clinical attention should be paid to increasing the strength of the denture, reducing the load in the premolar area, and reducing the stress on the abutment teeth.

Xu Jun [3] proposed placing a retention arm on the lingual side when repairing longitudinal dentition defects, which served the purpose of

Table 5. Statistical results

Dependent variable: VAR00003						
LSD						
(I) tissues	(J) tissues	Average difference (I-J)	Standard error	Significant	95% confidence interval	
					Upper limit	Lower limit
Implant (MPa)	Cortical bone (10-1 MPa)	-4.0468*	0.63657	0.000	-5.3469	-2.7468
	Cancellous bone (10-1 MPa)	-1.1157	0.63657	0.090	-2.4157	0.1844
	Mucosa stress (10-1 MPa)	-0.7502	0.63657	0.248	-2.0502	0.5499
	Mucosa displacement (10-3 MPa)	-0.1123	0.63657	0.861	-1.4124	1.1877
	Denture negative displacement (10-3 Mpa)	-0.3503	0.63657	0.586	-1.6504	0.9497
	Denture positive displacement (10-4 MPa)	-0.5673	0.63657	0.380	-1.8674	0.7327
Cortical bone (10-1 MPa)	Implant (MPa)	4.0468*	0.63657	0.000	2.7468	5.3469
	Cancellous bone (10-1 MPa)	2.9312*	0.63657	0.000	1.6311	4.2312
	Mucosa stress (10-1 MPa)	3.2967*	0.63657	0.000	1.9966	4.5967
	Mucosa displacement (10-3 MPa)	3.9345*	0.63657	0.000	2.6344	5.2346
	Denture negative displacement (10-3 Mpa)	3.6965*	0.63657	0.000	2.3964	4.9966
	Denture positive displacement (10-4 MPa)	3.4795*	0.63657	0.000	2.1794	4.7796
Cancellous bone (10-1 MPa)	Implant (MPa)	1.1157	0.63657	0.090	-0.1844	2.4157
	Cortical bone (10-1 MPa)	-2.9312*	0.63657	0.000	-4.2312	-1.6311
	Mucosa stress (10-1 MPa)	0.3655	0.63657	0.570	-0.9346	1.6656
	Mucosa displacement (10-3 MPa)	1.0033	0.63657	0.125	-0.2967	2.3034
	Denture negative displacement (10-3 Mpa)	0.7653	0.63657	0.239	-0.5347	2.0654
	Denture positive displacement (10-4 MPa)	0.5483	0.63657	0.396	-0.7517	1.8484
Mucosa stress (10-1 MPa)	Implant (MPa)	0.7502	0.63657	0.248	-0.5499	2.0502
	Cortical bone (10-1 MPa)	-3.2967*	0.63657	0.000	-4.5967	-1.9966
	Cancellous bone (10-1 MPa)	-0.3655	0.63657	0.570	-1.6656	0.9346
	Mucosa displacement (10-3 MPa)	0.6378	0.63657	0.324	-0.6622	1.9379
	Denture negative displacement (10-3 Mpa)	0.3998	0.63657	0.535	-0.9002	1.6999
	Denture positive displacement (10-4 MPa)	0.1828	0.63657	0.776	-1.1172	1.4829
Mucosa displacement (10-3 MPa)	Implant (MPa)	0.1123	0.63657	0.861	-1.1877	1.4124
	Cortical bone (10-1 MPa)	-3.9345*	0.63657	0.000	-5.2346	-2.6344
	Cancellous bone (10-1 MPa)	-1.0033	0.63657	0.125	-2.3034	0.2967
	Mucosa stress (10-1 MPa)	-0.6378	0.63657	0.324	-1.9379	0.6622
	Denture negative displacement (10-3 Mpa)	-0.2380	0.63657	0.711	-1.5381	1.0621
	Denture positive displacement (10-4 MPa)	-0.4550	0.63657	0.480	-1.7551	0.8451

Denture negative displacement (10-3 Mpa)	Implant (MPa)	0.3503	0.63657	0.586	-0.9497	1.6504
	Cortical bone (10-1 MPa)	-3.6965*	0.63657	0.000	-4.9966	-2.3964
	Cancellous bone (10-1 MPa)	-0.7653	0.63657	0.239	-2.0654	0.5347
	Mucosa stress (10-1 MPa)	-0.3998	0.63657	0.535	-1.6999	0.9002
	Mucosa displacement (10-3 MPa)	0.2380	0.63657	0.711	-1.0621	1.5381
	Denture positive displacement (10-4 MPa)	-0.2170	0.63657	0.736	-1.5171	1.0831
Denture positive displacement (10-4 MPa)	Implant (MPa)	0.5673	0.63657	0.380	-0.7327	1.8674
	Cortical bone (10-1 MPa)	-3.4795*	0.63657	0.000	-4.7796	-2.1794
	Cancellous bone (10-1 MPa)	-0.5483	0.63657	0.396	-1.8484	0.7517
	Mucosa stress (10-1 MPa)	-0.1828	0.63657	0.776	-1.4829	1.1172
	Mucosa displacement (10-3 MPa)	0.4550	0.63657	0.480	-0.8451	1.7551
	Denture negative displacement (10-3 Mpa)	0.2170	0.63657	0.736	-1.0831	1.5171

Based on measured mean. The error term is mean square=1.216. *The significance level of the mean difference is .05.

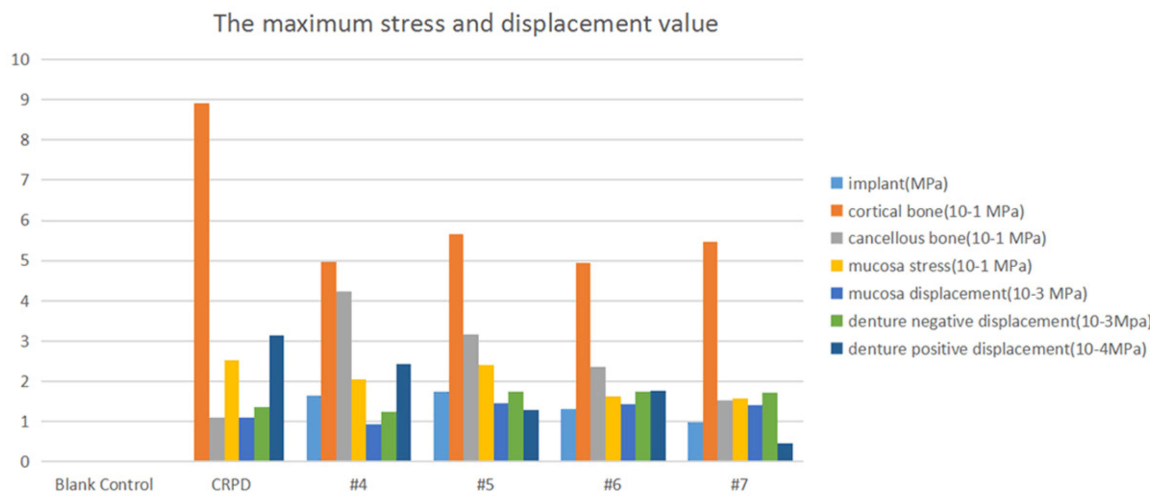

Figure 3. The Von Mises stress and displacement value.

protecting the abutment teeth. However, it effectively increases the burden of the mucous membrane and alveolar ridges. Hence, support is needed for the contralateral arch. The choices including using the residual roots of the sputum or using the implant to play a support role. The implant is then connected to the abutment and the denture for better rigidity support. The implants that simulate the residual roots also have a shorter interpupillary distance, and avoid the hidden danger of creating excessive lateral force due to poor crown/plant ratio, and provide a certain degree of protection for the implant. When international scholars [13] studied the retention structure above the implant, they found that the experimental group with a single fixed implant and a single crown supporting the CRPD produced significant displacement, and the implant bore an excessive load. Despite the limitations of that study, it still verified the possibility of failed osseointegration.

With the support of an implant, the stress on the alveolar ridge and the mucosa in the edentulous area are all less than that of the corresponding areas of the CRPD group, and the stress concentration area is still on the buccal side of the premolar zone. This is consistent with the findings of other scholars. When Ohkubo et al [18] studied Kennedy class-I distal implants used in support of RPDs, they found that the implantation of distal implants significantly reduced the pressure on the mucosa and the alveolar bone, and prevented the denture sinking among other instable phenomena. That same conclusion is also supported by a large number of clinical studies [15, 19]. The above observations suggest that implants with gaps produce effective support, reducing the pressure on the soft and hard tissues under the denture base, thus benefiting the health of these tissues.

The displacement of the denture shows that implant support significantly reduces tensile stress on the denture clasp, making the pressure more uniform, indicating that the implant's support changes the stress placed on the abutment teeth, reducing the effect on the anterior abutment teeth, and increasing the force on the posterior abutment teeth. Radwan [20] showed that the use of implants reduces the leverage of the distal denture base, and also reduces its effect on the abutment teeth. The shift from longitudinal support to flat support disperses the stress on each part and retains physiological stimulation while relieving stress, and is thus favorable for the healthy long-term development of tissues and abutment teeth.

Chikahiro [13] believed that because of the implant-bone bond, there is no periodontal ligament with a feedback mechanism, and that the load can neither be absorbed nor buffered. Thus, the ISRPD had a theoretically larger occlusal force than the CRPD. However, the results show that each organization has a tendency to reduce stress and distribute it more evenly, indicating that the implant bears most of the force and also changes the structure of the force transmission.

When implants are at different positions

In this experiment, the load is applied on the surfaces of all artificial teeth in a vertical, static, and even manner. Under the same load, given the stressed area of the premolar area is smaller than that of the molar area, the CRPD group had significantly higher stress on the alveolar bone in the premolar area and deformation of the mucosa than in the molar area. When implants are placed in the highly stressed area of the CRPD, the stress is greatly diluted and the uneven distribution is ameliorated. This situation had the shortest lever arm of force for its sinking effect and optimal supporting effects. As the implant moved towards the distal side, the lever arm of force gradually lengthened and gave gradually decreasing support to the premolar area. As a result, the Von Mises stress value of premolar area gradually increased. At the same time, the supporting role of the implant on the molar area gradually increased as it moved to the distal side. Although the degree was reduced, it still played a supporting role. The conclusions of the studies performed by Rocha et al. and Pellizzer et al [7, 19] suggested that the bonding of the implant and DERPD relieved the stress on the alveolar ridge, which consistent with the results of this experiment.

The implant endured more stress in the premolar area than in the molar area, indicating that in the premolar areas where the stress was concentrated, the implant bore most stress, thus reducing the load placed on the tissues. Yoshiki's [21] study on implant-assisted partial denture stress indicated that about half of the load is applied to the implant regardless of its position. Some scholars had come to different conclusions in this area. Cunha et al [18] observed the maximum stress of ISRPD implants and found that the implants had a positive effect on the stress distribution when they were closer to the abutment teeth. In the molar area where the stress concentration is relatively small, the implant is not stressed, but the cortical bone distributes more stress. This shows that, in the molar area, the implant is protected.

In terms of denture displacement, the denture base had a negative displacement value, suggesting that the denture base and tissues below it endured compressing stress, while the framework had a positive displacement value, indicating that the retainer on the abutment teeth is under tensile stress. With a supporting implant installed, the Stress on the retainer is significantly reduced, suggesting that the effect on the abutment is also alleviated. As the position of the implant moves distally, the difference between the mistal retainer and distal retainer is gradually reduced, and the distribution tends to be uniform. This indicates that placing implants in the molar region has a significant effect on optimizing the force placed on the abutment.

Conclusion

Within the scope of this experimental study, quantitative data of load distribution of denture, implant, alveolar ridge and mucosa were obtained with different implant distribution locations. The following conclusions are drawn from the results of this study: 1. The maximum stress of cortical bone, cancellous bone and mucous under the functional load of traditional longitudinal partial denture is concentrated on the buccal side of the premolar area. 2. The support of the implant reduces the burden on the abutment while making the occlusal force distribution more uniform. 3. The maximum stress of the implant is concentrated in the neck and 1/3 of the root. 4. In the premolar area, the implant effectively disperses the force and reduces the stress value of the cortical bone; in the molar area, the cortical bone takes more occlusal force and the implant is protected. [8, 16, 22-33]

Acknowledgements

We acknowledge the work of State Key Laboratory of Structural analysis for Industrial Equipment, Dalian University of Technology, Dalian, China (Item Number: GZ15206).

Disclosure of conflict of interest

None.

Address correspondence to: Yang Liu, Department of Prosthodontics, Dalian Stomatological Hospital, No.935 Changjiang Road, Shahekou District, China. Tel: 15524835176; Fax: 0411-84634970; E-mail: Liuyang913015@163.com

References

[1] Kelly E. Changes caused by a mandibular removable partial denture opposing a maxillary complete denture. J Prosthet Dent 1972; 27: 140-150.

[2] Yimin Z. Prosthodontics. People's Health Publishing House, 2012.

[3] Xujun. Design of full denture and removable partial denture. China Encyclopedia Publishing House, 2005.

[4] Giffin KM. Solving the distal extension removable partial denture base movement dilemma: a clinical report. J Prosthet Dent 1996; 76: 347-349.

[5] Keltjens HM, Kayser AF, Hertel R and Battistuzzi PG. Distal extension removable partial dentures supported by implants and residual teeth: considerations and case reports. Int J Oral Maxillofac Implants 1993; 8: 208-213.

[6] Lum LB. A biomechanical rationale for the use of short implants. J Oral Implantol 1991; 17: 126-131.

[7] Rocha EP, Luersen MA, Pellizzer EP and Del Belcury AA. Distal-extension removable partial denture associated with an osseointegrated implant. Study by the finite element method. Journal of Dental Research 2003; 82: B254-B254.

[8] Sato M, Suzuki Y, Kurihara D, Shimpo H and Ohkubo C. Effect of implant support on mandibular distal extension removable partial dentures: relationship between denture supporting area and stress distribution. J Prosthodont Res 2013; 57: 109-112.

[9] Witter DJ, De Haan AF, Käyser AF, Van Rossum GM. A 6 year follow up study of oral function in shortened dental arches PART II-craniomandibular dysfunction and oral comfort. J Oral Rehabil 1994; 21: 353-366.

[10] Pellecchia M, Pellecchia R, Emtiaz S. Distal extension mandibular removable partial denture connected to an anterior fixed implant-supported prosthesis: a clinical report. J Prosthet Dent 2000; 83: 607-612.

[11] Maeda Y, Sogo M and Tsutsumi S. Efficacy of a posterior implant support for extra shortened dental arches: a biomechanical model analysis. J Oral Rehabil 2010; 32: 656-660.

[12] Kordatzis K, Wright PS and Meijer HJ. Posterior mandibular residual ridge resorption in patients with conventional dentures and implant overdentures. Int J Oral Maxillofac Implants 2003; 18: 447-452.

[13] Ohkubo C, Kobayashi M, Suzuki Y and Hosoi T. Effect of implant support on distal-extension removable partial dentures: in vivo assessment. Int J Oral Maxillofac Implants 2008; 23: 1095-1101.

[14] Iplikçioğlu H, Akça K. Comparative evaluation of the effect of diameter, length and number of implants supporting three-unit fixed partial prostheses on stress distribution in the bone. J Dent 2002; 30: 41-46.

[15] Verri FR, Pellizzer EP, Rocha EP, Pereira JA. Influence of length and diameter of implants associated with distal extension removable partial dentures. Implant Dent 2007; 16: 270-280.

[16] Cunha LD, Pellizzer EP, Verri FR, Pereira JA. Evaluation of the influence of location of osseointegrated implants associated with mandibular removable partial dentures. Implant Dent 2008; 17: 278-287.

[17] Chou TM, Caputo AA, Moore DJ, Xiao B. Photoelastic analysis and comparison of force-transmission characteristics of intracoronal attachments with clasp distal-extension removable partial dentures. J Prosthet Dent 1989; 62: 313-319.

[18] Ohkubo C, Kobayashi M, Suzuki Y and Hosoi T. Effect of implant support on distal-extension removable partial dentures: in vivo assessment. Int J Oral Maxillofac Implants 2010; 34: 52-56.

[19] Lucas L, Pellizzer E, Rocha E and Pereira J. Avaliação da influência da força de mordida na prótese parcial removível classe I mandibular associada a implante, pelo método dos elementos finitos. Revista do Curso de Odontologia da UniEvangélica 2008; 10: 05-12.

[20] Hasan RH. Biomechanical assessment of implant supported removable partial denture: 3-D finite element analysis study. 2012.

[21] Matsudate Y, Yoda N, Nanba M, Ogawa T and Sasaki K. Load distribution on abutment tooth, implant and residual ridge with distal-extension implant supported removable partial denture. J Prosthodont Res 2016; 60: 282-288.

[22] Li Kai, Xin HT, Zhao YF, Zhang Q, Wu YL. Influence of implant number and location on the bone stress variation of mandibular implant supported overdentures. Clin Stomatol 2013; 29: 643-645.

[23] Becker W, Becker BE, Alsuwyed A and Al-Mubarak S. Long-term evaluation of 282 implants in maxillary and mandibular molar positions: a prospective study. J Periodontol 1999; 70: 896-901.

[24] Yanhua X. Analysis of jaw movement and biomechanical of oral and dental implant. 2017.

[25] Tong CH, Lv XF, Peng C. Effect of implant structural changes on the cortical bone stress distribution and peak of the implant-bone interface:a three-dimensional finite element analysis. Chinese Journal of Tissue Engineering Research 2015; 19: 1597-1602.

[26] Aunmeungtong W, Khongkhunthian P and Rungsiyakull P. Stress and strain distribution in

three different mini dental implant designs using in implant retained overdenture: a finite element analysis study. Oral Implantol (Rome) 2016; 9: 202-212.

[27] Zhang S, Fan R, Zheng YL. Stress analysis of the supporting tissues for mandibular kennedy class i defect repaired with removable partial dentures supported by implants. Journal of Shanghai Jiaotong University 2017; 37: 483-489.

[28] Cunha LD, Pellizzer EP, Verri FR, Falcón-Antenucci RM, Goiato MC. Influence of ridge inclination and implant localization on the association of mandibular kennedy class I removable partial denture. J Craniofac Surg 2011; 22: 871-875.

[29] Memari Y, Geramy A, Fayaz A, Rezvani Habib Abadi S, Mansouri Y. Influence of implant position on stress distribution in implant-assisted distal extension removable partial dentures: a 3D finite element analysis. J Dent (Tehran) 2014; 11: 523-530.

[30] Rodrigues RC, Faria AC, Macedo AP, de Mattos Mda G, Ribeiro RF. Retention and stress distribution in distal extension removable partial dentures with and without implant association. J Prosthodont Res 2013; 57: 24-29.

[31] Shahmiri R and Das R. Finite element analysis of implant-assisted removable partial dentures: framework design considerations. J Prosthet Dent 2017; 118: 177-186.

[32] Shahmiri R, Das R, Aarts JM and Bennani V. Finite element analysis of an implant-assisted removable partial dentureduring bilateral loading: occlusal rests position. J Prosthet Dent 2013; 22: 550-555.

[33] de Freitas RF, de Carvalho Dias K, da Fonte Porto Carreiro A, Barbosa GA, Ferreira MA. Mandibular implant-supported removable partial denture with distal extension: a systematic review. J Oral Rehabil 2012; 39: 791-798.